

IMECE2018-86222

IMPROVED NONLINEAR ULTRASONIC GUIDED WAVE DAMAGE DETECTION USING A BANDGAP META-SURFACE

Yiran Tian

UM-SJTU Joint Institute
Shanghai Jiao Tong University
Shanghai, China

Yanfeng Shen

UM-SJTU Joint Institute
Shanghai Jiao Tong University
Shanghai, China

ABSTRACT

In this study, a kind of meta-surface was designed for the improvement of nonlinear ultrasonic guided wave detection by creating bandgaps. It is composed of aluminum alloy cylinders arranged in a periodic pattern bounded on an aluminum plate. By artificially adjusting the height of the cylinders, the meta-surface can open up bandgaps over desired frequency ranges. Guided waves within the bandgap cannot propagate through the meta-surface and will be mechanically filtered out. To perform non-destructive evaluation (NDE) of structural components with fatigue cracks, the guided waves generated by a piezoelectric wafer active sensor (PWAS) propagate into the structure, interact with the crack, acquire nonlinear features, and are picked up by the receiver PWAS. In an ideal case, the waves excited by the transmitter PWAS should only contain signals at the fundamental frequency. However, due to the inherent nonlinearity of the electronic instrument, the generated signals are often mixed with weak superharmonic components. And these inherent higher harmonic signals will adversely affect the identifiability of nonlinear characteristics in the sensing signals. The bandgap mechanism and the wave vector dispersion relationship of the meta-surface are investigated using the modal analysis of a finite element model (FEM) by treating a unit structural cell with the Bloch-Floquet boundary condition. In this way, the meta-surface is carefully designed to obtain bandgaps at the desired frequency ranges. Then, a FEM harmonic analysis of a chain of unit cells is performed to further explore the bandgap efficiency. Finally, a coupled field transient dynamic FEM is constructed to simulate the improved nonlinear ultrasonic guided wave active sensing procedure with the bandgap meta-surface. The proposed method possesses great potential for future SHM and NDE applications.

INTRODUCTION

Mechanical Bandgap Metamaterial

The formation of bandgap characteristics based on local resonances has been investigated extensively in recent years. More and more researchers have paid attention to the design of metamaterial structures. Wu *et al.* proved the existence of complete bandgap and resonances in an aluminum plate with periodic stubbed surface. By adjusting the height of the stub, the desired frequency ranges over bandgaps can be achieved [1]. Oudich *et al.* designed a novel phononic crystal (PC) structure which is a thin homogeneous plate bounded by single-layer or two-layer stubs on the surface. They found the width of the bandgap can be enlarged by changing the height and the cross section area of the stubs [2]. To achieve lower frequency bandgap and confine energy propagation, Sun *et al.* utilized periodic circular membranes which have relatively weak rigidity property attached to the stubs to have slow propagating resonant modes [3]. Considering nonlinear damage detection, many researchers have put forward various methods to simulate it. Nonlinear ultrasonic technique using distinctive higher harmonics and subharmonics features, proves itself a promising approach to detecting structural damage [4-5]. Shen *et al.* presented a predictive modeling of nonlinear wave propagation for structural health monitoring with piezoelectric wafer active sensors. They proposed a Damage Index (DI) based on the amplitude ratio of the signal spectral harmonics to relate the signal nonlinearity with damage severity [6].

Nonlinear Sources of Ultrasonic NDE Waves

Guided waves have been investigated as a promising non-destructive testing tool because of their preferred features such as long propagation distance and sensitivity to a variety of structural damage types. The nonlinear ultrasonic technique has been reported to be more sensitive to incipient changes.

However, in experiments, even if the excitation signal only processes the fundamental frequency component, the nonlinear phenomenon can be observed before the guided waves interacting with the nonlinear damage in most cases for some reasons. This effect is not taken into account as usual, but it reduces the accuracy of the results. The nonlinear sources in practice can be divided into three categories: a) inherent nonlinearity of the electronic equipment; b) nonlinear property of the materials (the plastic property of the adhesive material bounded between sensors and the aluminum plate); c) nonlinear characteristics from the contact crack damage. During the tension and compression procedures, the linear relationship between stress and strain breaks down. To improve the diagnosis using the sensing signal, the effect of the first two sources should be minimized.

To demonstrate the first two nonlinear influence sources, a pristine aluminum plate with a transmitter PWAS and a receiver PWAS was tested. The T-PWAS was excited with a fundamental frequency signal at 50 kHz. The results are shown in Figure 1. Figure 1a shows the excitation signal generated from the function generator. The fundamental frequency of the sine signal is 50 kHz. Figure 1c shows the signal after the amplifier and

passing through the pristine aluminum plate. The higher harmonic features can be obviously observed. In this study, the focus is put on the fundamental frequency (50 kHz), the second harmonic (100 kHz) and the third harmonic (150 kHz). In order to make the simulation work approximate the reality, the amplitude ratios of higher harmonics components (100 kHz and 150 kHz) and the fundamental signal (50 kHz) are used in our model.

This paper focuses on using a kind of meta-surface to produce bandgap characteristics based on the principle of local resonances, leading to the filtration of guided waves over some spectral bands. This allows the diagnosis of nonlinear phenomena from contact dynamics stand out by diminishing the influence of inherent nonlinearity from electronic equipment and adhesive materials. It starts with the design and analysis of unit cell structure for bandgap meta-surface. Then the spectral response of the meta-surface will be further illustrated through harmonic analysis. Finally, a case study is presented with wave propagating in both pristine and damage plates. The improvement of nonlinear ultrasonic diagnosis capability is shown and discussed.

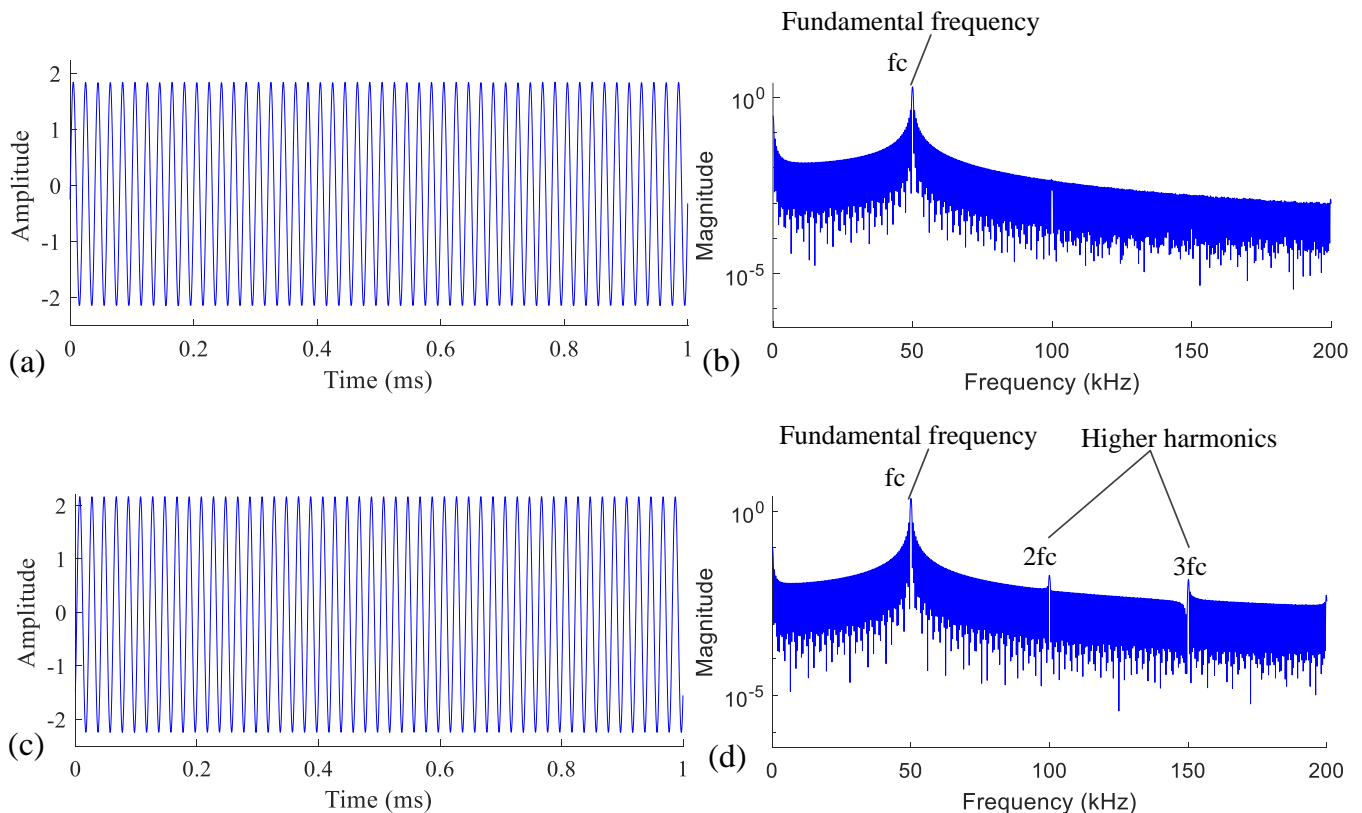


Figure 1: Signals from a pristine plate experiment: (a) time trace of the excitation signal; (b) frequency spectrum of the excitation signal; (c) time trace of the sensing signal; (d) frequency spectrum of the sensing signal

DISPERSION CURVE BANDGAP STRUCTURE OF METAMATERIALS

Standard Finite Element Formulation for Dispersion Curve Computation

The standard finite element method applies to the case that a harmonic wave propagates into a periodic material. By periodic, it is here meant that the material can be divided into finite-sized identical, so-called periodic cells [8]. Thus, one unit cell can represent the entire structure. By applying Bloch-Floquet, constraint equations to each point on the boundaries and the corners of the unit cell, the dispersion relation can be calculated. The dispersion curve represents the frequency

spectral in the wavenumber domain. By sweeping across the wavenumber domain, the natural frequencies corresponding to wave modes can be obtained rendering a frequency-wavenumber space. Based on the locally resonance (LR) mechanism [7], when the excitation frequency approaches to the resonant frequency of the meta-surface structure, the corresponding frequency will not be shown in the dispersion curve. Meanwhile, it means the guided waves under this frequency cannot pass through the structure and bandgaps develop. Figure 2 shows a unit cell after meshing in ANSYS package. In the next section, the dispersion curve of the unit cell based on this method will be presented.

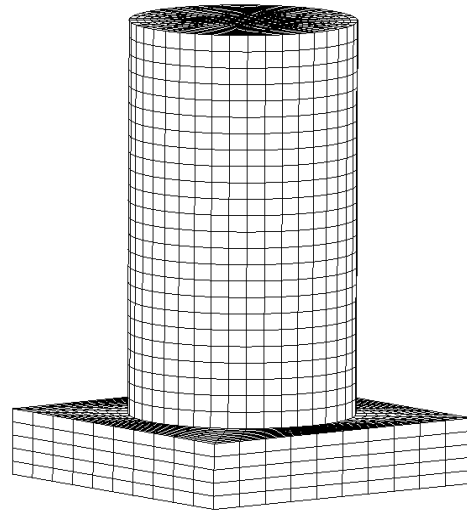


Figure 2: Meta-surface Unit Cell Finite Element Model

Dispersion Curves of Ultrasonic Meta-surface

Based on LR mechanism, we can design a unit cell to achieve the desired band gap frequency ranges. In this paper, the unit cell is constructed by a 2-mm thick aluminum plate and a certain height L of cylinder stub bounded on the plate. The radius r of the stub is 3.5-mm and the lattice constant a of the unit cell is 10mm. The dispersion curves of the unit cells with different heights of the stub are presented in Figure 3. Figure 3a shows the dispersion curve of a homogeneous 2mm-thick plate without a stub. It can be seen that no bandgaps appear in this case. Figure 3(b)–(d) show the dispersion curves of an aluminum plate with different heights of the stubs. By comparing the results, as the height of the stub increases, different numbers of bandgaps occurred in the dispersion curves. When the stub height is 6 times the plate thickness, three bandgaps in different frequency ranges appeared. When the height increased to 8mm, the bandgaps moved to lower ranges and a new one covering the higher frequency range appeared. However, when the height of the stub gradually

increased to 12mm, only a wide bandgap ranging from 86.56 kHz to 115.8 kHz was achieved. This bandgap frequency range can be used to filter out the superharmonic components shown in Figure 1d.

SPECTRAL RESPONSE OF THE META-SURFACE

Harmonic Analysis of Unit Cell Chain Model

Harmonic analysis was used to verify the results of the dispersing bandgap relationship. The structure was excited by a 50-N external force in frequency spectrum ranging from 0 to 250 kHz. The objective of using the model is to observe the displacement and equivalent stress responses of the structure under the excitation at different frequencies. Theoretically when the frequency range of the external force overlaps the bandgap, only the first few unit cells have the responses, while the rest unit cells seldom move, i.e., the guided wave cannot pass through the whole structure.

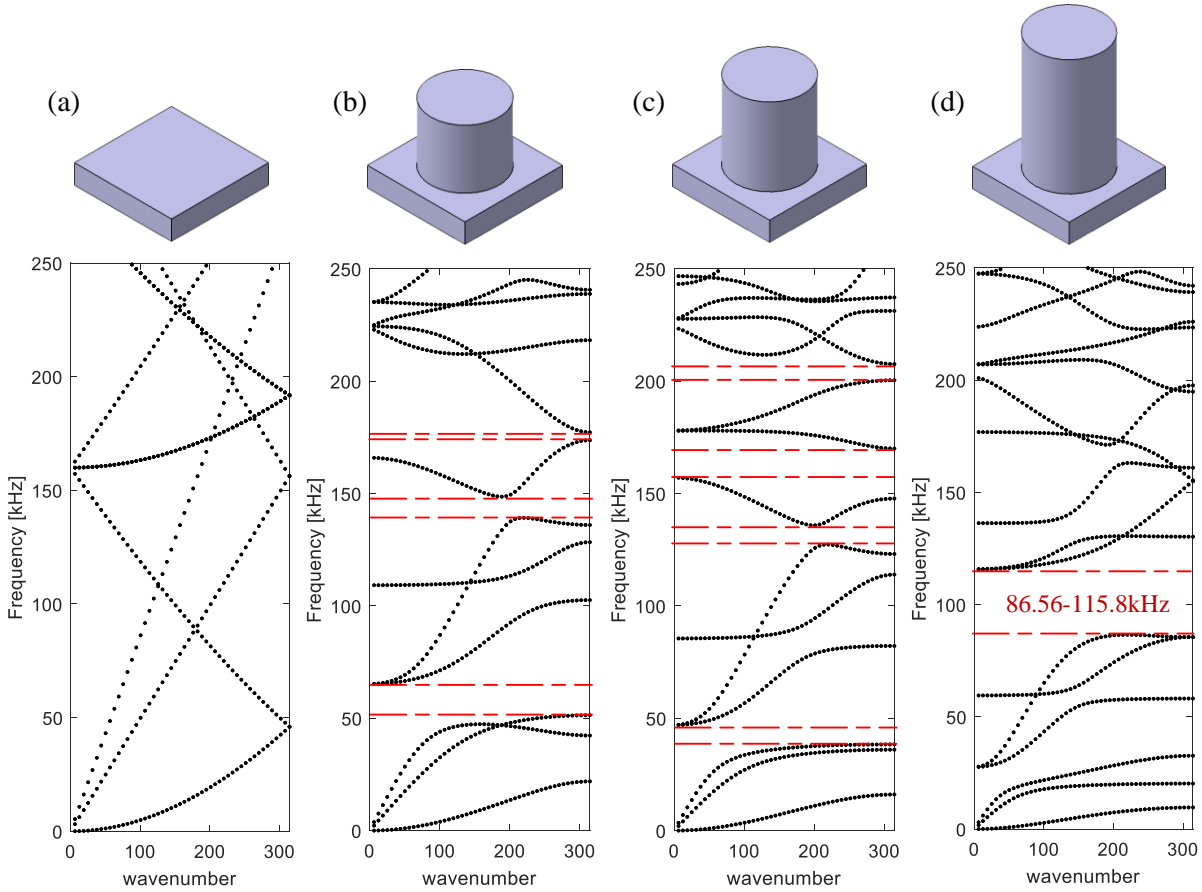


Figure 3: Unit cells with different heights of stubs and the dispersion curves obtained from modal analysis: (a) a homogeneous plate without stub; (b) a homogeneous plate with a 6-mm stub; (c) a homogeneous plate with an 8-mm stub; (d) a homogeneous plate with a 12-mm stub

Simulation Model and Results

Figure 4 shows the harmonic analysis results of the meta-surface. To demonstrate the bandgap behavior, a simple plate and a plate with the meta-surface were both simulated. The meta-surface structure contains an array of 10×1 unit cells (Figure 3d). The external force was applied on the left side of the structure, and the in-plane displacement of the point m on the right side of structure was calculated.

Figure 5 shows the in-plane displacement spectral response of point m. From the Figure 5a, it can be observed that the structure without the meta-surface responds with a large in-plane displacement under the excitation frequency from 86.56 kHz to 115.8 kHz. In comparison, the meta-surface structure has almost no response to the external force; after calculation, the in-plane displacement is in the order of $1E-7$ which can be ignored.

To illustrate the prowess of the meta-surface, the equivalent stress of the structure is also plotted. Figure 4(b)-(c) show the equivalent stress results of the homogeneous plate and the meta-surface with 12-mm high stub. Three frequencies

were calculated to show the equivalent stress of the structure, which are 80 kHz, 100 kHz and 200 kHz. 80 kHz frequency corresponds to a peak in the response spectrum under the bandgap shown in Figure 5b. 100 kHz is the frequency within the bandgap. 200 kHz is the frequency out of the bandgap, but the in-plane displacement of the structure is also small. From the results, the equivalent stress of the two structure are both very large under 80 kHz excitation. When the frequency of the external force increases to 100 kHz, the homogeneous aluminum structure still has a large amplitude. However, only the first three unit cells of the structure with the meta-surface show obvious oscillation and the equivalent stresses are also very small. For 200 kHz, it can be seen that even if the in-plane displacement of the meta-surface structure is small, all the unit cells are excited by the external force, which means the guides waves still can propagate through the meta-surface structure.

Above all, the results from the harmonic analysis agree well with the bandgap feature. It can be concluded that 100 kHz cannot propagate through the proposed meta-surface.

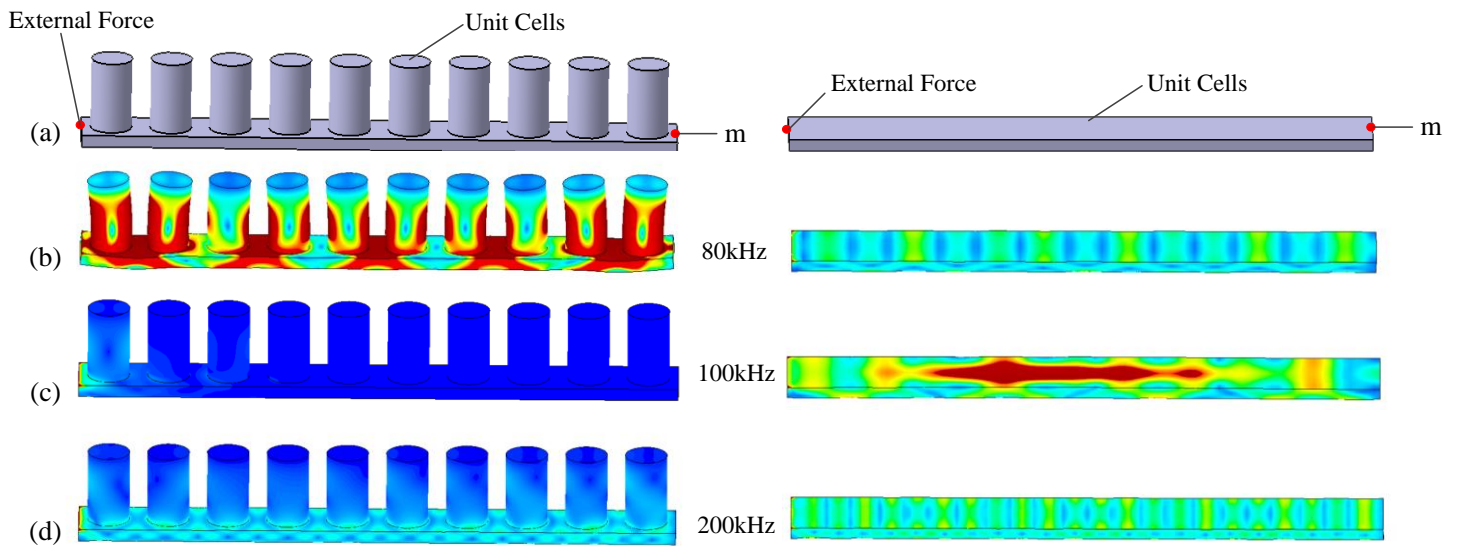


Figure 4: The designed structure with an array of 10×1 unit cells and the equivalent stress under different frequencies: (a) the meta-surface structure and a simple plate strip; (b) wavefield at 80 kHz; (c) wavefield at 100 kHz; (d) wavefield at 200 kHz

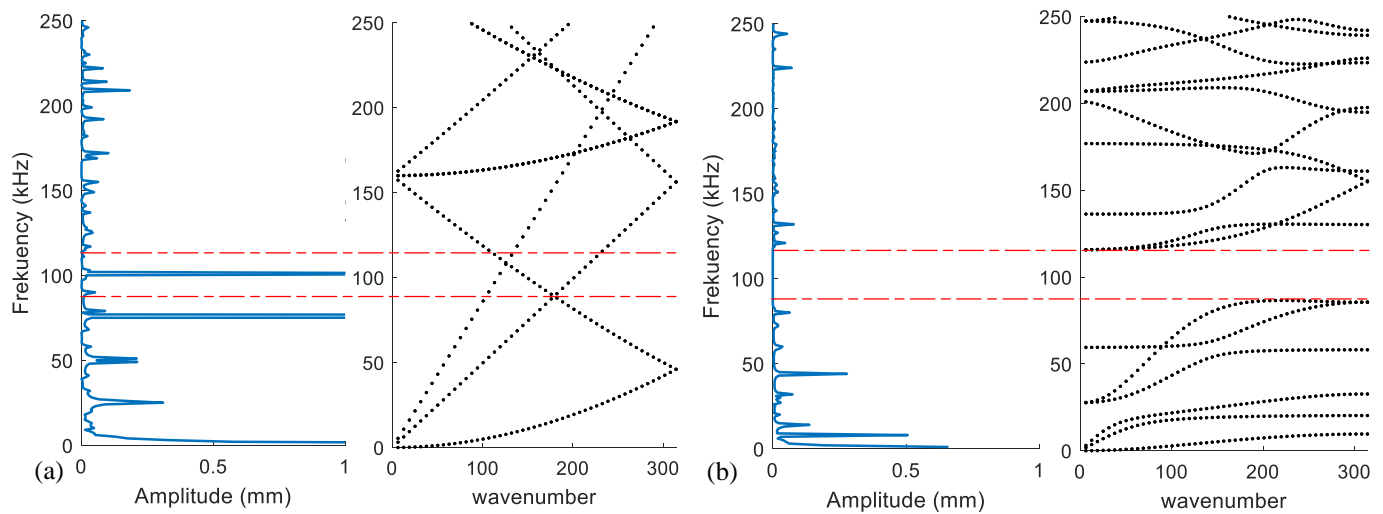


Figure 5: The results comparison between modal analysis and harmonic analysis: (a) the simple plate case; (b) the case with 12-mm stub meta-surface

TRANSIENT DYNAMIC FINITE ELEMENT MODELING OF NONLINEAR ULTRASONIC NDE

Superharmonic Response of Wave Crack Nonlinear Interaction

After the guided waves interacting with the crack, higher harmonic components may appear in the receiving signals. The

phenomena of higher harmonic generation can be illustrated in a simple way by using a general nonlinear dynamic system [9-11].

$$U = Ax(1 + \beta x + \gamma x^2 + \dots) \quad (1)$$

Where U is the output of the system, A is a scale factor, and β and γ are the second and third nonlinear coefficients. Consider a harmonic input

$$X(\omega) = \hat{x} \cdot e^{i\omega t} \quad (2)$$

By substituting equation (2) into equation (1), the output of the nonlinear system takes the form

$$\begin{aligned} U &= A\hat{x}e^{i\omega t} + A\beta(\hat{x}e^{i\omega t})^2 + A\gamma(\hat{x}e^{i\omega t})^3 + \dots \\ &= A\hat{x}e^{i\omega t} + A\beta\hat{x}^2e^{2i\omega t} + A\gamma\hat{x}^3e^{3i\omega t} + \dots \\ &= AX(\omega) + A\beta\hat{x} \cdot X(2\omega) + A\gamma\hat{x}^2 \cdot X(3\omega) + \dots \end{aligned} \quad (3)$$

Equation (3) shows that the output of the nonlinear system contains higher harmonics 2ω , 3ω , and ... while the input to the system contains only one frequency allows us to detect material degradation, fatigue, micro cracks, or state of clamping surfaces, which introduce nonlinearity to structures [6].

Finite Element Modeling of Nonlinear Ultrasonic

Figure 6 shows the model layout of a pitch-catch NDE procedure using the meta-surface. One 10-mm×5-mm×0.2-mm rectangular PWAS was bounded on the left side of a 2mm-thick aluminum plate to generate guided waves. Another circular PWAS with a 3.5-mm radius and 0.2-mm thickness was bounded on the right side of the aluminum plate to receive the signals. The crack was located at 130-mm from the transmitter behind the meta-surface. An array of 10×1 meta-surfaces was bounded on the homogeneous aluminum plate. The circular receiver PWAS was located on the right side of the crack at a 15-mm distance. Non-reflective boundaries (NRB) were implemented on both ends of the plate strip to avoid the influence from boundary reflections. The transmitter PWAS would generate ultrasonic guided waves into the structure, carrying both the fundamental frequency waves (50 kHz) and superharmonic components (100 kHz, 150 kHz, etc.)

from the inherent nonlinear sources. The waves would propagate through the meta-surface, undergo bandgap filtration diminishing the second harmonic participation at 100 kHz. The guided waves would further interact with the crack, carrying crack information with them, and finally picked up by the receiver PWAS.

PWAS transducers were modeled with the coupled field elements (SOLID5) which couple the electrical and mechanical variables. The three-dimensional structure was modeled with four-node structural element SOLID45. A 100vpp 40-count tone burst signal centered at 50kHz with inherent superharmonic components at 100kHz and 150kHz was applied on the top electrode of the transmitter PWAS.

To ensure the accuracy of the results and solve the problem more efficiently, the element size and the time step should be optimized. The maximum acceptable element size and time step are governed by the following equations [9]

$$l_e = \frac{\lambda_{\min}}{20} \quad (4)$$

$$\Delta t = \frac{1}{20f_{\max}} \quad (5)$$

where λ_{\min} is the minimum wavelength, f_{\max} is the maximum frequency, l_e is the maximum acceptable element size and Δt is the time step.

The minimum wave length was evaluated via the dispersion curves of the plate following Eq. (6)

$$\lambda = \frac{c}{f} \quad (6)$$

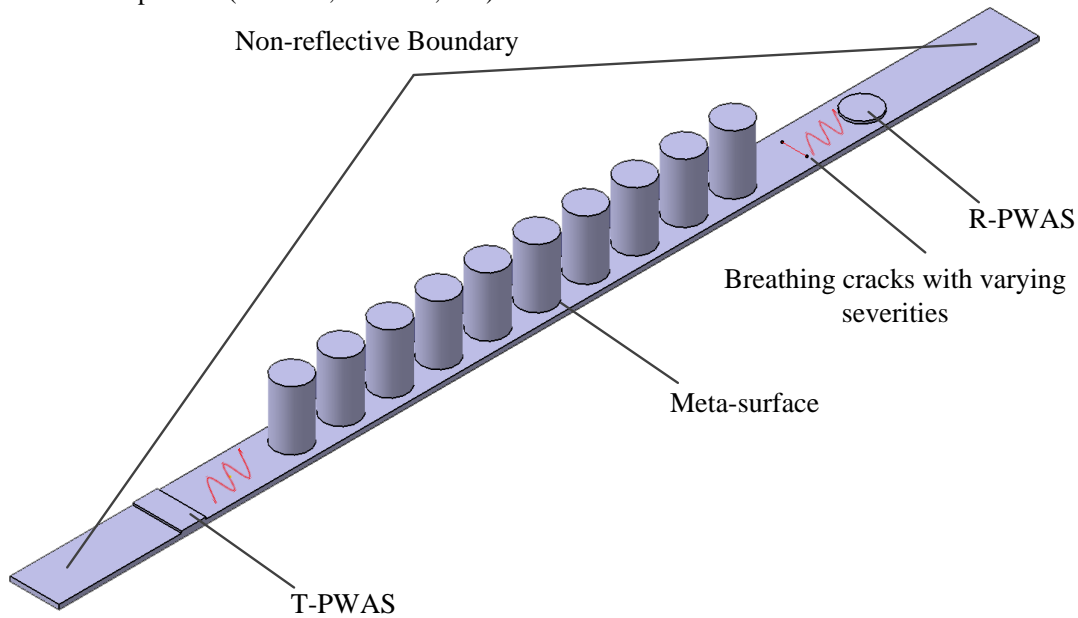


Figure 6: Model layout of a pitch-catch nonlinear ultrasonic NDE procedure with the meta-surface

The wave speed can be calculated by solving the Rayleigh-Lamb equation and shown in Figure 7a. The wavelength is plotted in Figure 7b. From the figure, A0 mode at 150 kHz possesses the minimum wavelength 10.32-mm. According to the equation (5) and (6), the maximum element size vs frequency and time step vs frequency relationships are respectively shown in Figure 7c and Figure 7d. At higher harmonic frequency (150 kHz), the maximum mesh size is 0.5161-mm. So in our model, the maximum element size was set to be 0.5-mm to

guarantee the space discretization requirement. From the Figure 7d, the maximum allowable time-step is 0.33 μ s. To satisfy the condition, the time-step in our model was set to be 0.3 μ s. The guided wave has A0, S0 and SHS0 modes at the fundamental frequency (50 kHz). However, only A0 and S0 modes need to be considered. The length of the non-reflective boundary should be twice as long as the maximum wavelength. Hence, the length of the non-reflective boundary was set to 40-mm.

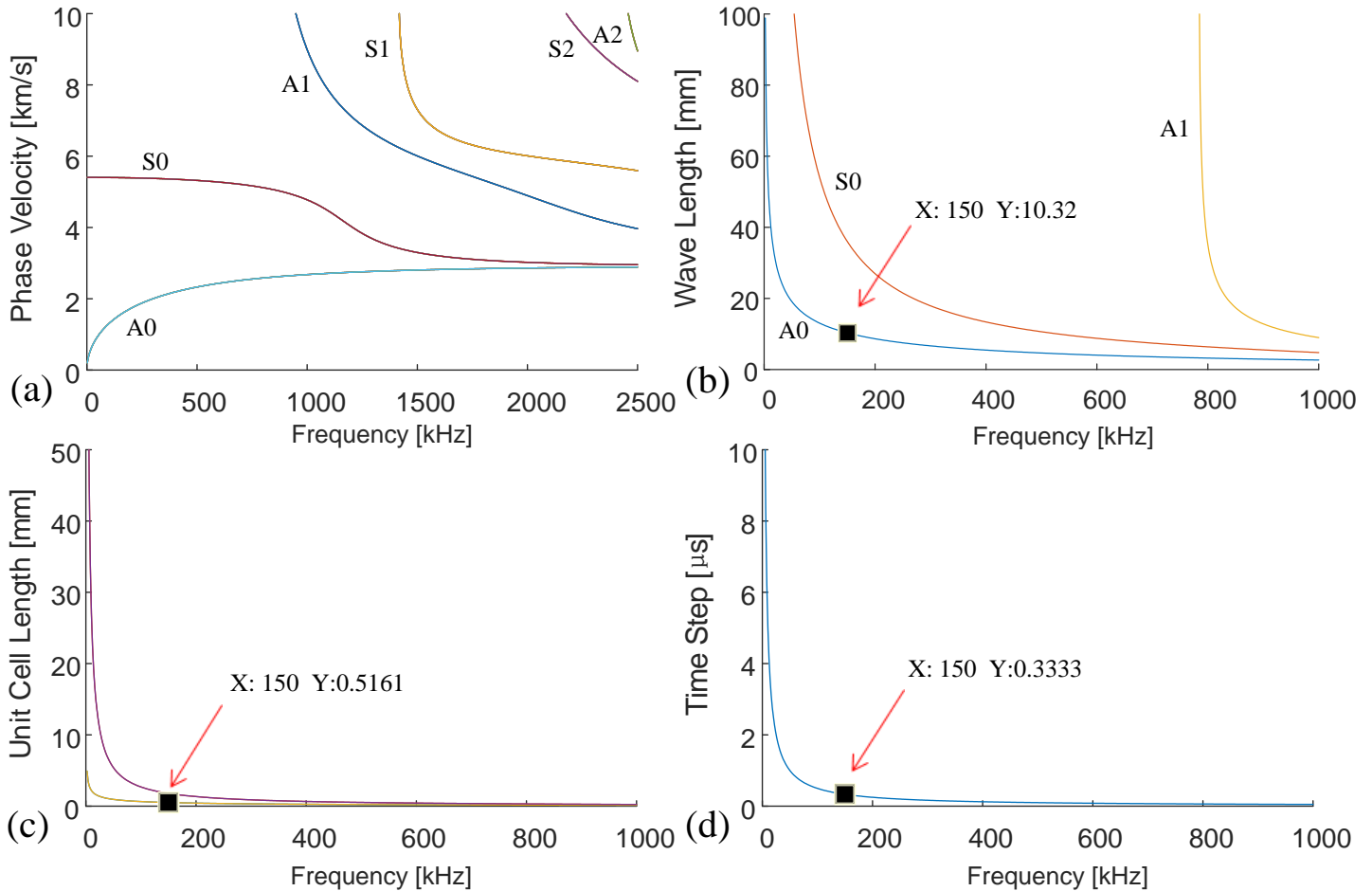


Figure 7: Discretization guideline figures: (a) phase velocity dispersion curves; (b) wavelength dispersion curves; (c) frequency element size curve; (d) frequency time step curve

CASE STUDY

This section presents the modeling results using transient dynamic analysis for the simulation of nonlinear ultrasonic NDE pitch-catch active sensing procedure. Figure 8 shows the time trace of the excitation and sensing signals. The frequency spectrum of the excitation signal with three components at the frequency of 50 kHz, 100 kHz and 150 kHz. Figure 8d presents the frequency spectrum of the wave signal received by R-PWAS. Figure 9 illustrates the short-time Fourier transform

(STFT) of the excitation and receiving signals through PWAS. It is obvious that in addition to the fundamental frequency and third higher harmonics, the second higher harmonic was filtered away. Such nonlinear higher component brings complexity in analyzing the nonlinearity from the NDE signal. The meta-surface has the ability of filtering out the inherent nonlinearity of the electronic instruments which is evidently shown in Figure 9b. This will make the nonlinear phenomenon of the contact crack more clear and accurate.

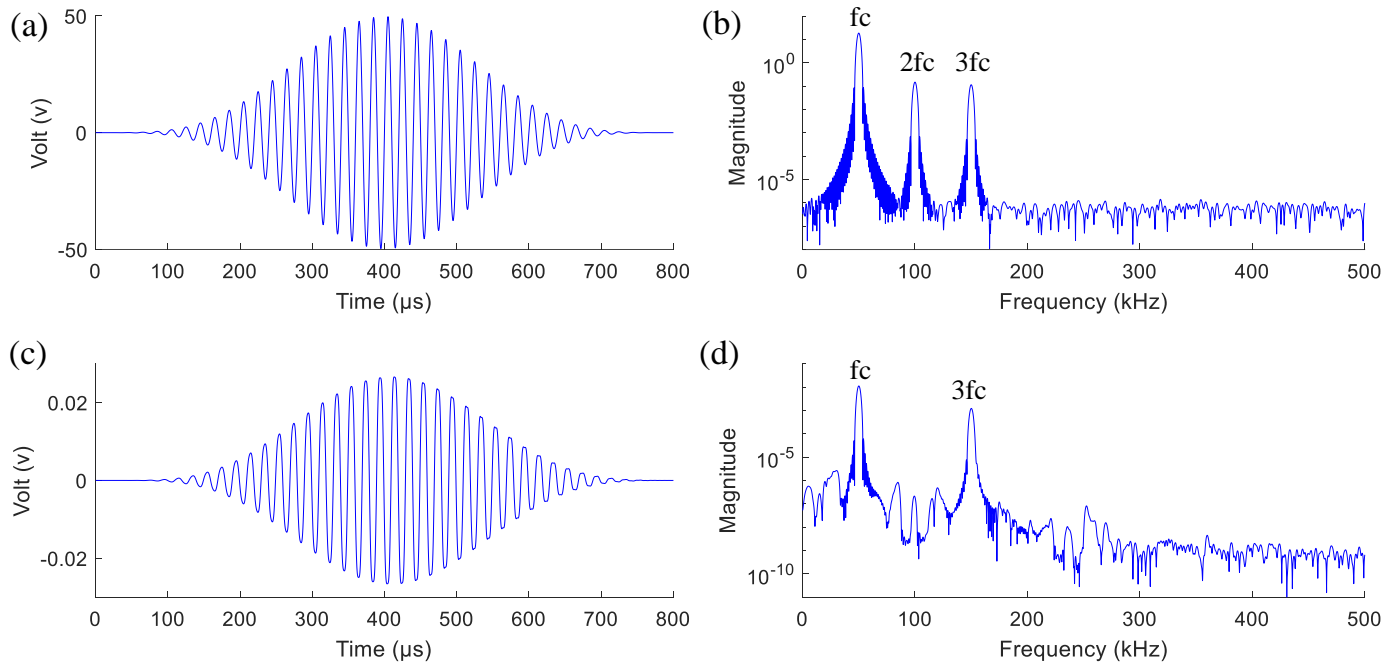


Figure 8: Pitch-catch NDE Signals: (a) time trace of the excitation; (b) frequency spectrum of the excitation; (c) time trace of the sensing signal; (d) frequency spectrum of the sensing signal

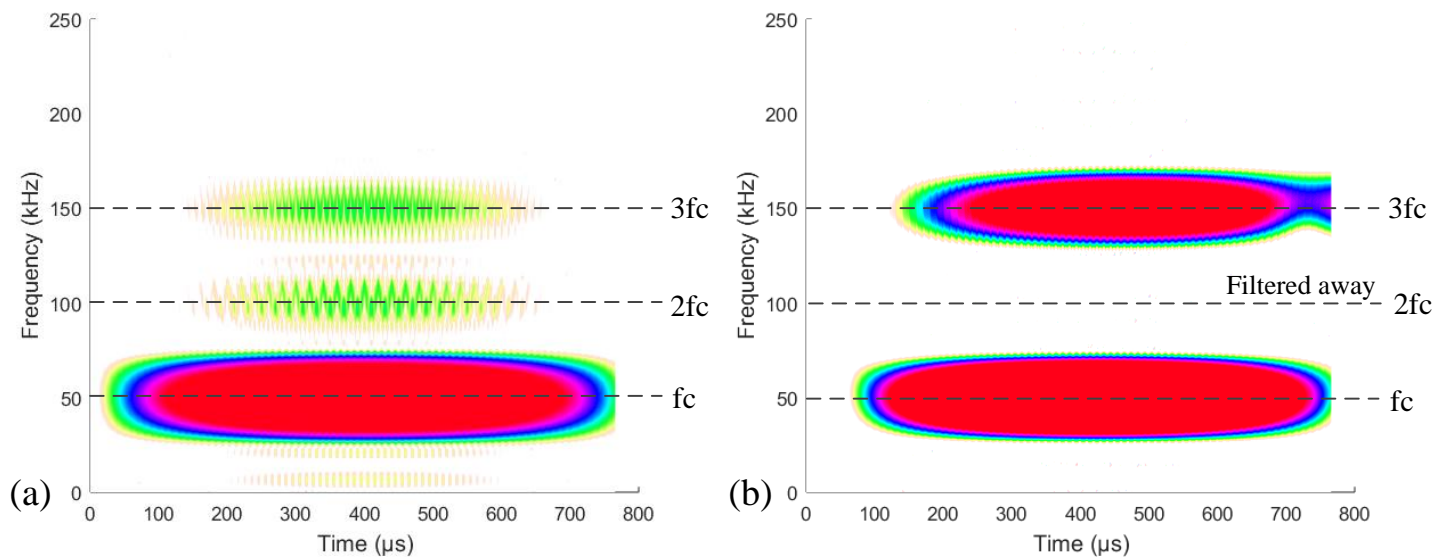


Figure 9: Short-time Fourier transform of signals: (a) excitation signal; (b) receiving signal

CONCLUDING REMARKS

In this paper, a new concept of using meta-surface for the improvement of nonlinear ultrasonic NDE was put forward. A bandgap meta-surface was designed with periodically arranged unite cells. This kind of meta-surface can filter out the second harmonic component (100 kHz) introduced by the inherent

nonlinearity of the electronic instruments. By artificially adjusting the height of the stubs, bandgaps can be created to render different filtering frequency ranges. As the height of the stubs increased, the bandgaps moved to lower frequency ranges.

Harmonic analysis was performed to obtain the spectral response of the meta-surface. The bandgap feature was further

demonstrated. Within the bandgap, the wave dynamics only existed in the first few unit cells. The guided waves at such frequency would not propagate through the meta-surface.

A case study of pitch-catch nonlinear ultrasonic NDE procedures was modeled. Inherent superharmonics were included in the excitation signal, simulating the participation of various nonlinear sources in practice, such as those from the electronic device and the adhesive layers. The bandgap range was set to the second harmonic location around 100 kHz. It was found that the inherent second harmonic was effectively removed from the interrogating wave signal, leaving merely the fundamental excitation and the third higher harmonic. Such phenomena helps to improve the identifiability of nonlinearity from wave crack interactions. Continuing work is being conducted, simulating the pitch-catch wave propagation through a breathing crack. The key results will be added in the paper revision stage and will be presented at the conference. The proposed method may find its great potential in future SHM and NDE applications.

ACKNOWLEDGMENTS

The support from the National Natural Science Foundation of China (contract number 51605284) is thankfully acknowledged.

REFERENCES

- [1] Wu, T.T.; Huang, Z.G.; Tsai, T.C.; Wu, T.C. (2008), "Evidence of complete band gap and resonances in a plate with periodic stubbed surface", *Applied Physics Letters* 93, 111902 (2008)
- [2] Mourad, O.; Li, Y.; Badreddine, M.A.; Hou Z.L. (2010), "A sonic band gap based on the locally resonant phononic plates with stubs", *New Journal of Physics*, 12 083049
- [3] Sun, C.Y.; Hsu, J.G.; Wu T.T. (2010), "Resonant slow modes in phononic crystal plates with periodic membranes", *Applied Physics Letters* 97, 031902 (2010)
- [4] Jhang, K.Y. (2009), "Nonlinear ultrasonic techniques for nondestructive assessment of micro damage in material: a review", *International Journal of Materials* 10: 123-135
- [5] Kruse, W.; Zagrai, A. (2009), "Investigation of linear and nonlinear electromechanical impedance techniques for detection of fatigue damage in aerospace materials", In: *7th international workshop on structural health monitoring*, Stanford, CA, 9-11 September
- [6] Shen, Y.; Giurgiutiu, V. (2014), "Predictive modeling of nonlinear wave propagation for structural health monitoring with piezoelectric wafer active sensors", *Journal of Intelligent Material Systems and Structures*, Vol. 25, pp. 506-520
- [7] Zhu, R.; Liu, X.N.; Hu, G.K.; Yuan, F.G.; Huang, G.L. (2015), "Microstructural designs of plate-type elastic metamaterial and their potential applications: a review", *International Journal of Smart and Nano Materials*, 6:1, 14-40, DOI: 10.1080
- [8] Aberg, M; Gudmundson .P, (1997) "The usage of standard finite element codes for computation of dispersion relations in materials with periodic microstructure", *Acoustical Society of America*. 102, (1997); doi: 10.1121/1.419652
- [9] Hagedorn, P.; (1988) "Nonlinear Oscillations", *New York: Oxford University Press*
- [10] Lee, T.H.; Choi, I.H. (2008) "The nonlinearity of guided waves in an elastic plate", *Modern Physics Letter* 22:1135-1140
- [11] Naugoslnykh, K.; Ostrovsky, L. (1998) *Nonlinear Wave Processes in Acoustic*, Cambridge, MA: Cambridge University Press